JOURNAL OF APPLIED ELECTROCHEMISTRY 20 (1990) 17–22

The effect of nickel on the mechanism of the initial stages of zinc electrowinning from sulphate electrolytes. Part II. Investigations on aluminium cathodes alloyed with iron impurities

CHR. BOZHKOV*, M. PETROVA, ST. RASHKOV

Institute of Physical Chemistry, Bulgarian Academy of Sciences, 1040 Sofia, Bulgaria

Received 3 January 1989; revised 21 March 1989

The effect of the alloying element Fe on the electrochemical behaviour of Al cathodes during the initial stages of zinc electrowinning was studied, using scanning electron microscopy, cyclic voltammetry, atomic absorption and X-ray microprobe analysis techniques. It is shown that underpotentially deposited zinc submonolayer inhibits the discharge of hydrogen ions onto Fe aggregates – alloying element.

1. Introduction

It was shown in Part I (this issue, p. 11) that when spectral grade Al is used, the conditions under which the initial stages of Zn nucleation, and H_3O^+ discharge proceed exert a definite effect upon the structure and properties of zinc deposits obtained in sulphate electrolytes. Under these conditions the simultaneous codeposition of Ni^{2+} and Zn^{2+} strongly catalyses the H_3O^+ reduction and conditions are created for the formation of active regions (free of Zn deposits) with respect to hydrogen bubbles on the Al cathode.

However the Al cathodes currently used in the industrial Zn electrowinning process have a purity grade of about 99.6%, containing several alloying elements, most commonly Fe, Cu, Zn, Si, Pb, Mn, etc., iron, as a rule, being present in amounts of approximately 0.2%.

A detailed survey of the literature shows that while the effect of electropositive metal impurities in working electrolytes has been studied with great interest [1–5], similar investigations concerning the influence of alloying metals in the Al cathodes are lacking. This is probably due to the fact that at working current densities of about 5 A dm^{-2} the aluminium cathode is completely covered with zinc during the initial 3–4 min of the electrowinning process and the effect of the impurities in the electrolyte should be considered upon a continuously renovated Zn surface. In spite of this, when the zinc deposit is stripped off the aluminium cathode during electrowinning in Ni^{2+}-containing electrolytes, dark regions of the cathode side are clearly visible. This means that the processes occurring during the initial stages are involved in the structural peculiarities of the entire deposit [6].

Taking into consideration that iron has electrochemical properties similar to Ni with respect to the hydrogen discharge reaction [7, 8] and also that the amount of iron in the Al cathode substrate is much higher (~ 0.2%) than the bulk concentration of Ni^{2+} in the electrolyte, it should be expected that its effect during the initial stages would be predominant.

The present paper is aimed at the clarification of the problems concerning the consecutive ordering and the mechanism of electrochemical processes during zinc deposition from sulphate electrolytes under the conditions of the concurrent deleterious effect of Ni^{2+} in the electrolyte and Fe-phase in the surface layer of the aluminium cathode.

2. Experimental

The experimental conditions were similar to those described in Part I.

The cathodes were prepared from thin Al metal sheet (0.5 mm) supplied by Riedel-de Haën (Cat. No. 11003) with a geometrical surface area of 1 cm^2. The impurity content in the Al was determined by emission spectral analysis and the data are shown in Table 1. The composition of the impurities in the zinc deposits was determined with the aid of a Perkin Elmer atomic absorption analyser and microprobe X-ray spectral analysis (Superprobe 733 – JEOL). Parallel cyclic voltammetry investigations were carried out upon spectral purity grade iron and nickel cathodes (Johnson Matthey).

3. Experimental results

Figures 1 and 2 shows the (I–E) relationships obtained at different $ZnSO_4$ concentrations in Ni^{2+}-free electrolytes (Fig. 1) and containing 10 mg l^{-1} Ni^{2+} (Fig. 2).

* Author to whom correspondence should be addressed.

0021-891X/90 $03.00 + .12

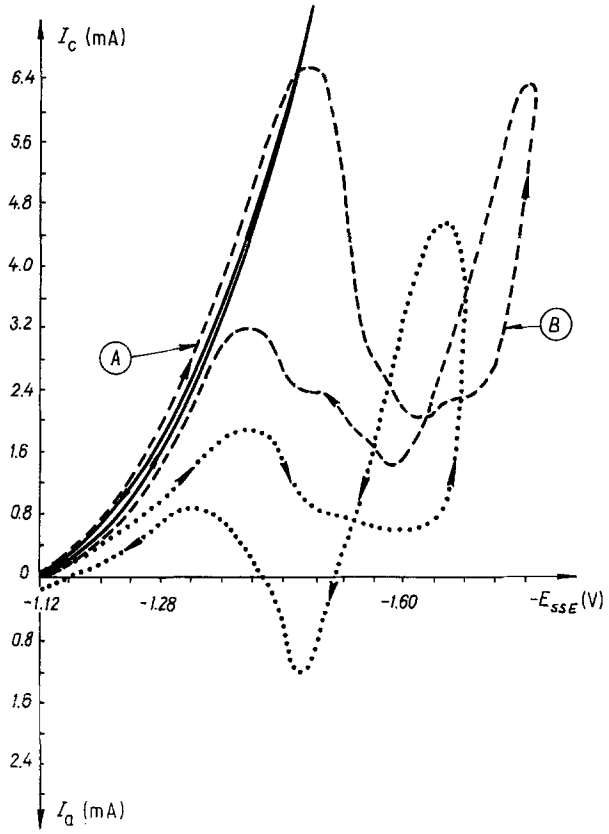

Fig. 1. Cyclic voltammograms traced at pH × 0.2 and sweep rate $W = 50\,\text{mV min}^{-1}$ in electrolytes containing: (——) supporting (Zn^{++}-free) electrolyte; (– – –) 0.01 M $ZnSO_4$; (· · · ·) 0.1 M $ZnSO_4$.

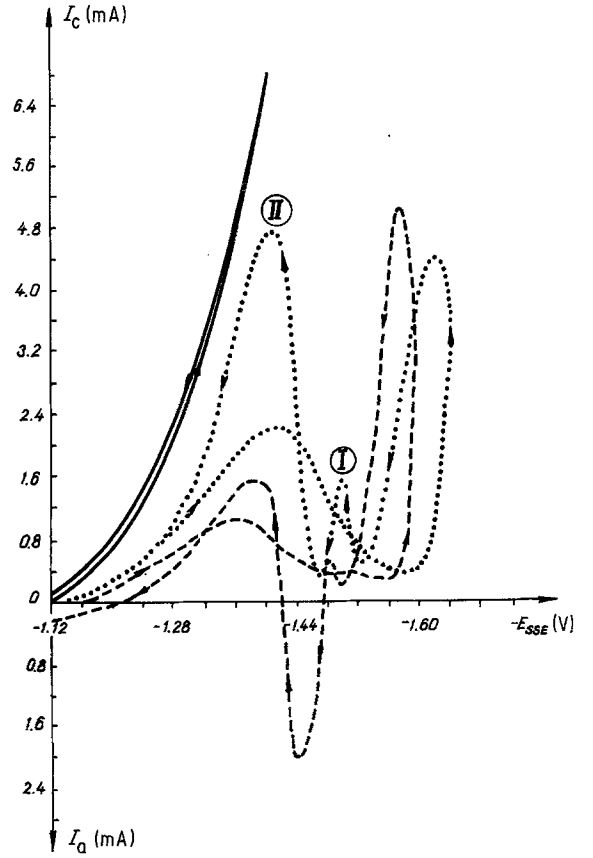

Fig. 2. Cyclic voltammograms traced at pH = 0.2 and sweep rate $W = 50\,\text{mV min}^{-1}$ in electrolytes containing $10\,\text{mg l}^{-1}$ Ni^{++}: (——) supporting (Zn^{++}-free) electrolyte; (· · · ·) 0.5 M $ZnSO_4$; (– – –) 1 M $ZnSO_4$.

It may be noted in Fig. 1 that the curves have a completely different shape to those obtained upon a spectral purity grade aluminium – (see Fig. 1, Part I). The difference at potentials more positive than $-1.5\,V_{SSE}$ is very pronounced. Within this region a

Table 1. Emission spectral analysis of the aluminium for impurity content data.

Element	*Accuracy [%]*	*Quantity [%]*	
		Practical used Al	*Riedel-de Haën*
Al		⩾3 base	⩾3 base
Zn		⩽0.01	⩽0.1
Fe		⩽0.3	⩽0.3
Si		⩽0.3	⩽0.3
Na	0.03	–	–
K	0.3	–	–
Cu		⩾0.0003	⩾0.0003
Mg		⩾0.001	⩾0.001
Ca	0.001	–	–
Ba	0.01	–	–
Ti		≃0.01	⩾0.01
Sn	0.001	–	–
Pb		⩾0.003	⩾0.003
Cr	0.001	⩾0.001	⩾0.003
Mn		⩾0.001	⩽0.01
V		⩾0.001	⩾0.001
Co	0.001	–	–
Ni	0.001	–	–
Ga		≃0.03	≃0.03
B	0.001	⩾0.001	–

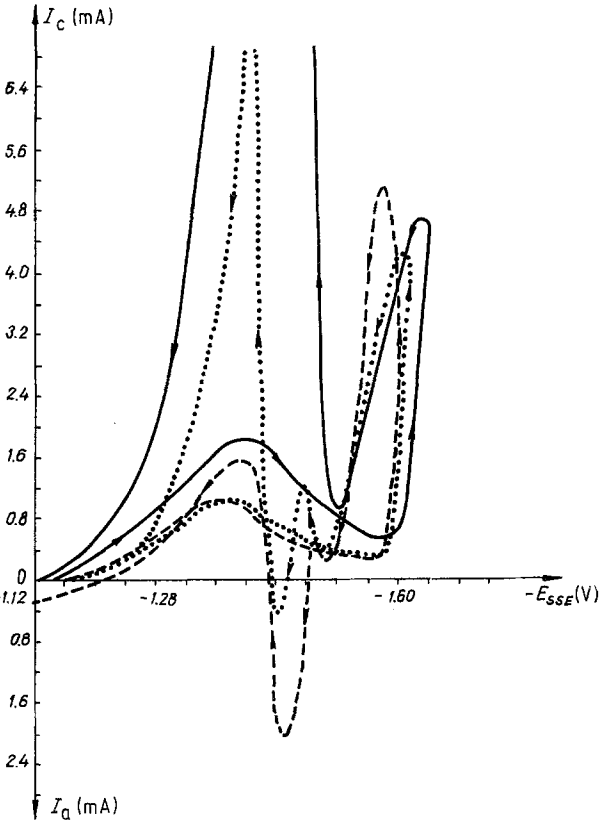

Fig. 3. Cyclic voltammograms traced at pH = 0.2 and sweep rate $W = 50\,\text{mV min}^{-1}$ in electrolytes containing: (——) 0.5 M $ZnSO_4$ and $30\,\text{mg l}^{-1}$ Ni^{++}; (– – –) 1.0 M $ZnSO_4$ and $10\,\text{mg l}^{-1}$ Ni^{++}; (· · · ·) 1,0 M $ZnSO_4$ and $30\,\text{mg l}^{-1}$ Ni^{++}.

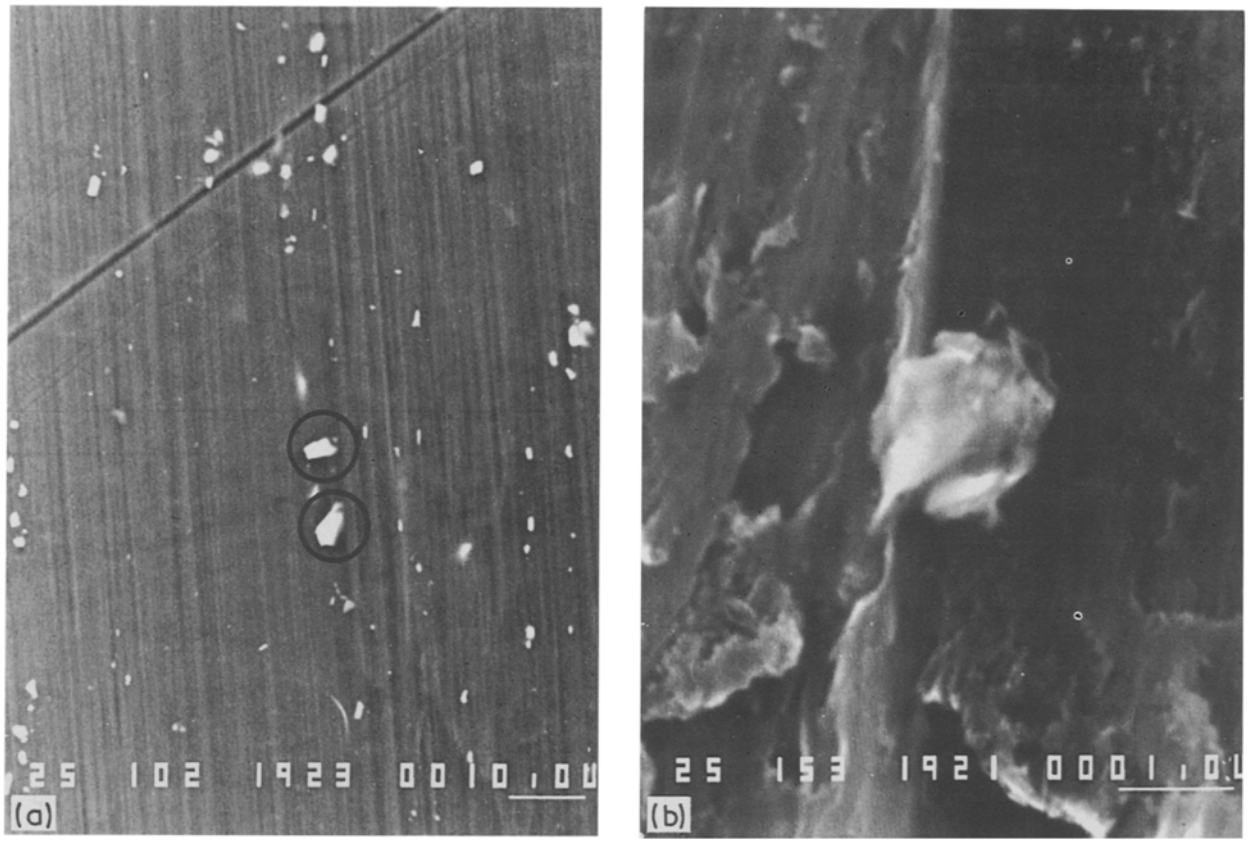

Fig. 4. SEM – microphotographs showing the typical morphology of Al-cathodes before deposition of Zn. (a) before mechanical polishing, (b) after mechanical polishing.

decreasing current maximum can be observed as the concentration of the Zn-salt is increased which, in the initial region of low concentration, completely coincides with the current curve of the supporting electrolyte, obtained in the absence of Zn^{2+}. Similar current relationships have been reported by several authors [4, 9–12] and the nature of this current maximum has been found to be the result of a 'contact adsorption' of Zn^{2+} onto Al [10, 13, 14].

In the presence of $10\,mg\,l^{-1}$ Ni^{2+} (Fig. 2), in the anodic scan region and at potentials more positive than $-1.5\,V_{SSE}$, two cathodic maxima are again observed, similar to those established on spectral purity grade Al (Fig. 2, Part I).

The similarity in both cases is that when the scan is over, at $E = -1.20\,V_{SSE}$ the cathodic current coincides with the value obtained in the Zn^{2+}-free supporting electrolyte. This is a characteristic difference as compared with the relationships obtained with Al cathodes (Johnson Matthey).

The dependence of I_{max} and II_{max} (Fig. 2) on the Ni^{2+} and Zn^{2+} concentrations (Fig. 3) is similar to that established in Part I.

These current maxima increased abruptly at higher Ni^{2+} concentrations, the second maximum (II_{max} – the more positive) being more sensitive, while higher $ZnSO_4$ concentrations suppress them. This phenomenon has provided grounds for some authors [4, 15] to propose the height of II_{max} as a quantitative measure for the determination of Ni^{2+} concentration in the electrolyte.

Obviously the difference in the ($\dot{I}$–E) relationships obtained with Riedel-Al and Johnson Matthey-Al is due to the difference in their chemical composition. This becomes clearer from the electron micrographs of the Riedel Al cathodes (Fig. 4). The results of the microprobe spectral analysis shown in Fig. 5 were obtained upon different sites of the cathode surface and they provide unambiguous evidence that the light regions in Fig. 4 are Fe-phases with a mean size of 1.0 to 1.5 μm. In this case it is natural that the current

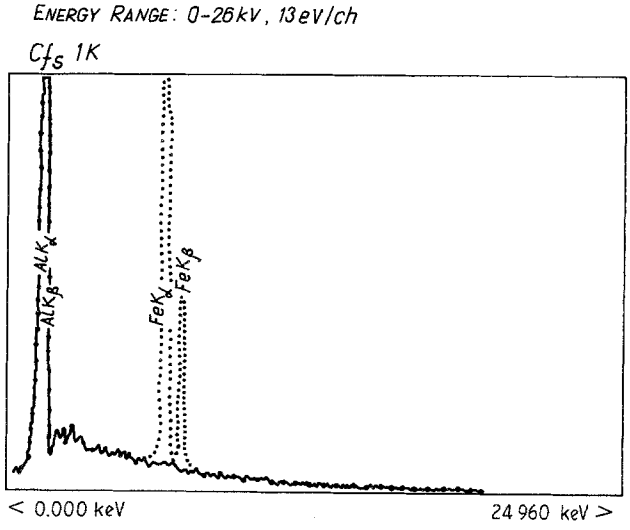

Fig. 5. X-ray microprobe analysis spectras obtained on the light (1) and dark (2) regions in Fig. 4.

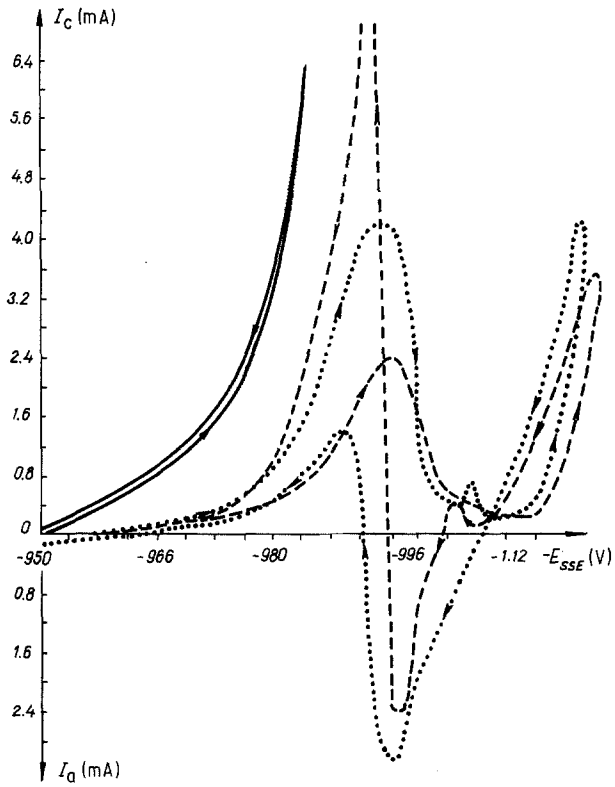

Fig. 6. Cyclic voltammograms traced at pH = 0.2 and sweep rate $W = 50\,\text{mV min}^{-1}$ upon a spectral pure Fe-cathode: (——) supporting (Zn^{++}-free) electrolyte; (· · ·) 0.5 M $ZnSO_4$; (– – –) 0.5 M $ZnSO_4$ with $10\,\text{mg l}^{-1}$ Ni^{++}.

measured at potentials more positive than $-1.4\,V_{SSE}$ should be related to the participation of Fe-aggregates in the electrochemical process. This is clearly backed by the shape of the (I–E) curves obtained with spectral grade (Johnson Matthey) Fe cathodes, (Fig. 6), which, in the initial regions, coincide with the curves obtained using Riedel aluminium substrates.

An important problem still remains, however, concerning the nature of this electrochemical process, i.e. whether this is only a discharge of H_3O^+, or whether, at potentials which are much more positive than the Nernst potential of Zn, the discharge of Zn^{2+} also participates, as suggested by the investigations of O'Keefe [10] and Maja [13, 14].

Some characteristic features of the electrochemical process can be established from the (I–E) relationships obtained under different conditions: of pH, Zn^{2+} and Ni^{2+} concentrations and scan rate W.

The current relationships obtained at different pH values, (Fig. 7), lead to the conclusion that the hydrogen reaction is catalysed more than with the spectral purity grade Al, which is quite natural if we accept that part of the aluminium cathode at these potentials behaves as an iron electrode. This effect is further enhanced by the presence of Ni^{2+}.

The strong dependence of the entire (I–E) curve on the scan rate (Fig. 8) reflects the irreversible electrochemical discharge and ionization stages, both of Zn^{2+} and Ni^{2+}, since in this case the rate determining stage of Ni^{2+} is involved, which, for its part, catalyses the reduction of H_3O^+. The rate of the latter process should not depend on W, at least up to $W \leqslant 100\,\text{mV s}^{-1}$ [16].

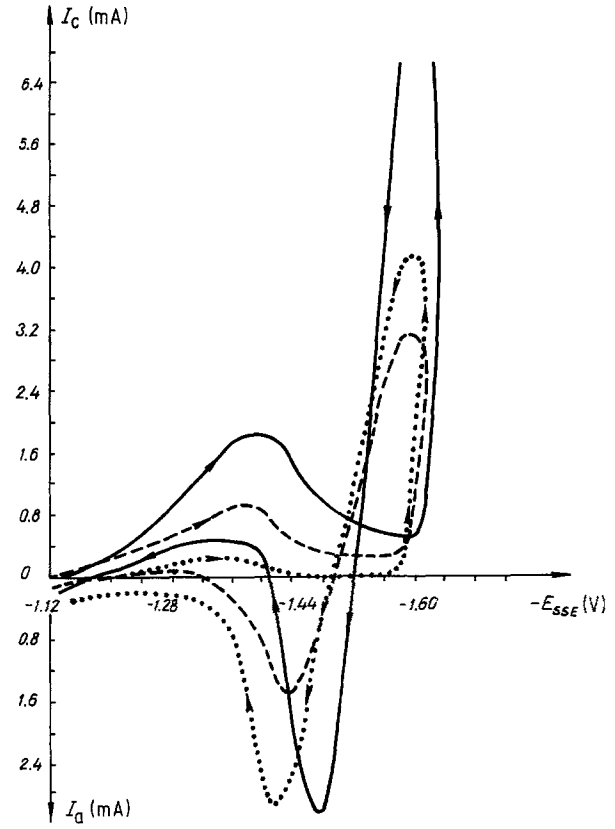

Fig. 7. Cyclic voltammograms traced in electrolytes containing 0.5 M $ZnSO_4$ at $W = 50\,\text{mV min}^{-1}$ and different pH: (——) pH = 0.2; (– – –) pH = 0.5; (· · ·) pH = 1.0.

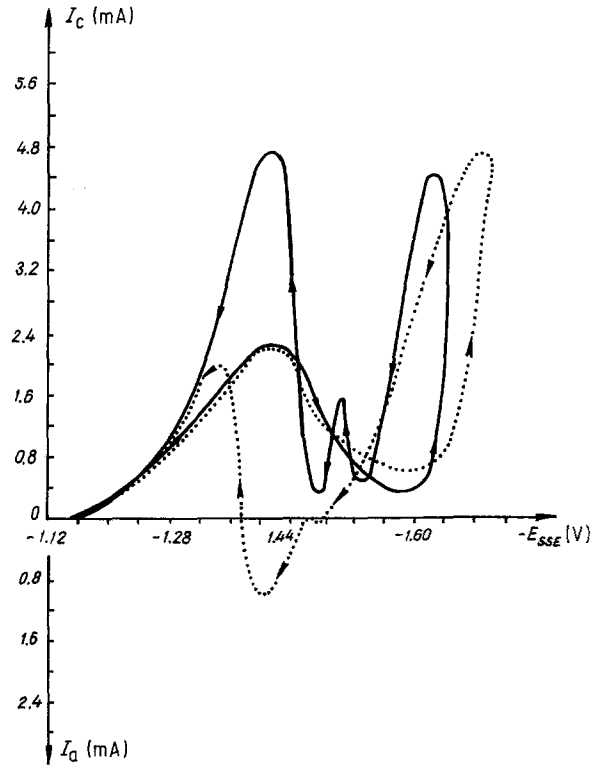

Fig. 8. Cyclic voltammograms traced in electrolytes containing 0.5 M $ZnSO_4$ and $10\,\text{mg l}^{-1}$ Ni^{++} at pH = 0.2 and different scanning rates: (——) $W = 50\,\text{mV min}^{-1}$; (· · ·) $W = 200\,\text{mV min}^{-1}$.

Table 2. Atomic absorption data of the deposits obtained under potentiostatic conditions

Electrolyte	E (*V*)	*Zn* (*g*)	*Ni* (*g*)	*Mn* (*g*)
H_2SO_4, $MnSO_4$, $ZnSO_4$	−1.36	1.4×10^{-5}	–	7.7×10^{-7}
	−1.43	1.15×10^{-5}	–	–
	−1.53	1.07×10^{-3}	–	–
H_2SO_4, $MnSO_4$, $ZnSO_4$, Ni^{2+}–9 mg l^{-1}	−1.36	3.8×10^{-5}	1.18×10^{-6}	6.9×10^{-6}
	−1.43	3.6×10^{-5}	3.6×10^{-5}	7.44×10^{-6}
	−1.53	8.7×10^{-4}	1.13×10^{-6}	9.6×10^{-4}

4. Discussion

The characteristic shape of the (*I–E*) relationships in Fig. 1, with a current maximum at potentials more positive than the Zn deposition value, has been comprehensively discussed in several investigations [10–14]. Thus, one of the explanations relates this current maximum to the inhibition of the discharge rate of the hydrogen ions as a result of the 'contact adsorption' of Zn^{2+} onto Al, which occurs at potentials more positive than the Nernst value for Zn. This is evident, since the polarization curve obtained in the supporting electrolyte gradually changes its character and slope as the concentration of the Zn salt increases (Fig. 1).

The contradiction in this case, however, is in the fact that according to the well known Klob–Gerisher relationship [17] concerning the underpotential behaviour of metal pairs:

$$\Delta E_{UPD} = 0.5\Delta\phi \qquad (1)$$

a similar process of underpotential deposition of Zn^{2+} onto Al is impossible, owing to the reverse work function difference ($\Delta\phi$) of the metals ($\phi_{Al} \leqslant \phi_{Zn}$) [18].

In order to provide more information, detailed investigations were carried out using atomic absorption and X-ray spectral microprobe analysis of the qualitative and quantitative composition of deposits obtained under potentiostatic conditions. The cathodic scan was stopped at potentials: $E = -1.36$, -1.43 and $-1.53\,V_{SSE}$ for $t = 2$ to 5 min and the deposit covering electrode was subjected to these investigations. Similar tests were carried out in the presence of 9 mg l^{-1} Ni^{2+} in the electrolyte.

These studies suggest that at the potentials of the adsorption current maximum ($E \sim -1.40$ V) (Figs 1 and 2) the atomic absorption analysis shows the presence of deposited Zn as well as Ni (Table 2). In our opinion this is a fact of major importance, since under these conditions the alloying element (Fe) determines the electrochemical behaviour of the Al cathode. According to the empirically established Kolb–Gerisher relationship [17] underpotential deposition (UPD) of Zn^{2+} onto Fe-substrates is possible ($\phi_{Fe} > \phi_{Zn}$) at: $\Delta E_{UPD} \sim 150$ mV. A similar UPD of Zn^{2+} upon ARMCO – Fe membranes was established by us recently in another study [19]. Thus, in this way, the results presented in Fig. 1 can be rationalized.

Keeping in mind that nickel should be deposited predominantly at potentials more positive than $E = -1.43\,V_{SSE}$, it was interesting to check whether its discharge is localized only on the Fe phase or also on the Al surface, as established in Part I. Microprobe studies were carried out for this purpose with samples deposited at $E = -1.36\,V_{SSE}$ and $E = -1.43\,V_{SSE}$ from electrolytes containing different Ni^{2+} concentrations up to 30 mg l^{-1}. It was established that Ni^{2+} is deposited mainly upon the Fe aggregates. This, in turn, determines the local discharge of H_3O^+, i.e. mainly onto the Fe phase, and the local formation of hydrogen bubbles on these sites. These active sites, as we will show in a following paper [20] become pitting defects.

5. Conclusion

The voltage–current, electron microscopic, atomic absorption and X-ray investigations at different pH, Ni^{2+} and Zn^{2+} content provide unambiguous evidence that the codeposition of Ni^{2+} and Zn^{2+} strongly catalyse the discharge rate of H_3O^+. It has been established that a process of underpotential deposition of Zn^{2+} occurs on the Fe impurities present in the Al as aggregates, while in the presence of Ni^{2+} in the electrolyte, nickel is predominantly deposited upon these active sites, creating conditions for the formation of gaseous hydrogen.

It may be concluded that the pitting defects are formed early in the initial stages of zinc deposition, which is determined mainly by the depolarization effect of the metal impurities in the surface layer of the Al cathode. In comparison with the latter, the effect of Ni^{2+} in the electrolyte is insignificant.

In a following paper [20] we will provide data about the relationship between the size of the pitting defect, determined by the shape of the hydrogen bubble and its wetting angle with the substrate, and the duration of the 'induction period'.

Acknowledgements

The authors are indebted to Professor R. Wiart, Paris, for helpful discussion of the results of this investigation.

References

[1] U. Turomshina and V. Stender, *J. Appl. Chem. USSR* **28** (1955) 151; **28** (1955) 372; **28** (1955) 447.

[2] D. Fosnach and T. O'Keefe, *J. Appl. Electrochem.* **10** (1980) 495.
[3] M. Maja, N. Penazzi, R. Fratesi and G. Roventi, *J. Electrochem. Soc.* **129** (1982) 2695.
[4] D. Mackinnon, R. Morrison and J. Brannen, *J. Appl. Electrochem.* **16** (1986) 53.
[5] M. Jaksić, *Surface Technology* **24** (1985) 95; **28** (1986) 113; **29** (1986) 95.
[6] I. Epelboin, M. Ksouri and R. Wiart, *Faraday Symp. Chem. Soc.* **12** (1977) 10.
[7] M. Jaksić, *Electrochim. Acta* **29** (1984) 1539.
[8] N. Shohoji, *Surface Technology* **28** (1986) 365.
[9] B. Lamping and T. O'Keefe, *Metallurgical Transactions* **7B** (1976) 551.
[10] Yar-Ming Wang, T. O'Keefe and W. James, *J. Electrochem. Soc.* **127** (1980) 2589.
[11] R. Singh and T. O'Keefe, *J. Electrochem. Soc.* **132** (1985) 2898.
[12] D. Mackinnon, J. Brannen and P. Fenn, *J. Appl. Electrochem.* **17** (1987) 1129.
[13] R. Fratesi, G. Roventi, M. Maja and N. Penazzi, *J. Appl. Electrochem.* **10** (1980) 765.
[14] M. Maja, N. Penazzi, R. Fratesi and G. Roventi, *J. Electrochem. Soc.* **129** (1982) 2695.
[15] R. Kerby, *UK Patent* 2024865 A (1978).
[16] F. Woodard, M. Hanafey and C. Reilley, *J. Electroanal. Chem.* **167** (1984) 43, 65.
[17] D. Kolb, M. Przasnyski and H. Gerisher, *J. Electroanal. Chem.* **54** (1974) 25.
[18] S. Trasatti, *J. Electroanalyt. Chem.* **33** (1971) 351.
[19] St. Rashkov, Chr. Bozhkov, V. Kudrijavtsev, K. Pepan and S. Bagaev, *J. Electroanalyt. Chem.* **248** (1988) 421.
[20] Chr. Bozhkov, St. Rashkov, R. Wiart and C. Cachet, *J. Appl. Electrochem.* (in press).